Biosensors and Bioelectronics 87 (2017) 850–857

Contents lists available at ScienceDirect

Biosensors and Bioelectronics

journal homepage: www.elsevier.com/locate/bios

Thiamine biosensor based on oxidative trapping of enzyme-substrate intermediate

Matilte Halma[a,b], Bastien Doumèche[c], Laurence Hecquet[a,b], Vanessa Prévot[a,b], Christine Mousty[a,b,*], Franck Charmantray[a,b,*]

[a] Clermont Université, Université Blaise Pascal, Institut de Chimie de Clermont-Ferrand, BP 10448, F-63000 Clermont-Ferrand, France
[b] CNRS, UMR 6296, ICCF, F-63171 Aubière, France
[c] ICBMS (Institut de Chimie et Biochimie Moléculaires et Supramoléculaires) UMR 5246 CNRS, Université Lyon 1, France

ARTICLE INFO

Keywords:
Thiamine
Biosensor
Transketolase
Layered double hydroxides
Hexacyanoferrate

ABSTRACT

In the present work, we describe a new thiamine amperometric biosensor based on thiamine pyrophosphate (ThDP)-dependent transketolase (TK)-catalyzed reaction, followed by the oxidative trapping of TK intermediate α,β-dihydroxyethylthiamine diphosphate (DHEThDP) within the enzymatic active site. For the biosensor design purpose, TK from *Escherichia coli* (TK*ec*) was immobilized in $Mg_2Al\text{-}NO_3$ Layered Double Hydroxides (LDH) and the electrochemical detection was achieved with the TK*ec*/LDH modified glassy carbon electrode (GCE). The transduction process was based on the ability of $Fe(CN)_6^{3-}$ to oxidize DHEThDP to glycolic acid along with ThDP regeneration. The released $Fe(CN)_6^{4-}$ was re-oxidized at +0.5 V *vs* Ag-AgCl and the reaction was followed by chronoamperometry. The TK*ec*/LDH/GCE biosensor was optimized using the best TK donor substrates, namely L-erythrulose and D-fructose-6-phosphate. ThDP was assayed with great sensitivity (3831 mA M^{-1} cm^{-2}) over 20–400 nM linear range.

1. Introduction

Vitamin B_1, also known as thiamine, is a biological and pharmaceutically important compound present in natural nutriments. Since humans (or mammals) cannot synthesize or meaningfully store thiamine, an essential nutriment in human diet, an adult should ingest a daily dose of 1.1–1.4 mg of thiamine (Butterworth, 2003; Isenberg-Grzeda et al., 2012; Smithline et al., 2012).

In vivo, thiamine diphosphate (ThDP), the phosphorylated analog of thiamine, is the biological active and circulating form of vitamin B_1. It is a cofactor of several enzymes involved into the carbohydrate metabolism (Basiri et al., 2016; Isenberg-Grzeda et al., 2012; Lonsdale, 2006; Rahman et al., 2015; Smithline et al., 2012). For instance, ThDP is the cofactor of transketolase (TK; EC 2.2.1.1), a key enzyme of the non-oxidative branch of the pentose phosphate pathway (Meshalkina et al., 2010; Ranoux and Hanefeld, 2013; Sprenger, et al., 1995). TK catalyzes the stereospecific formation of a C–C bond by the reversible transfer of the C1-C2 ketol unit from a ketose phosphate to an aldose phosphate. Thiamine deficiency causes reduced TK activity that triggers severe pathologies such as cancer (Ahopelto et al., 2016; Bentz et al., 2013; Du et al., 2004; Xu et al., 2016), diabetes (Michalak et al., 2013; Zhao and Zhong, 2009); heart failure (Hanninen et al., 2006) and several nervous system diseases such as Beriberi (Butterworth, 2003; Lonsdale, 2006), Wernicke-Korsakoff syndrome (Butterworth, 2003; Isenberg-Grzeda et al., 2012; Lonsdale, 2006; Wang et al., 2007) and Alzheimer disease (Karuppagounder et al., 2009; Mocali et al.; 2014).

Hence, the determination of vitamin B_1 in clinical samples, in food and pharmaceutical formulations is of high interest. Different analytical approaches such as spectrophotometry (Li et al., 2013; Moghaddam et al., 2014; Parsaei et al., 2014; Tan et al., 2015), high performance liquid chromatography (Basiri et al., 2016; Hanninen, et al., 2006; Poongothai et al., 2010) and detection by electrochemistry (Akyilmaz et al., 2006; Akyilmaz and Yorganci, 2008; Oni et al., 2002; Parshina and Bobreshova, 2014; Tyszczuk-Rotko, 2012; Wan et al., 2002) have being widely used for quantitative determination of thiamine from different sources (blood, urine, food, pharmaceutical tablets). These methods usually suffer from low-sensitivity or require sophisticated and expensive instrumentation that prevents their use in routine experiments.

Alternatively, biosensors are of great concern for the quantification of an analyte of interest. Because of their high sensitivities and specific activities, enzymes are mainly used in biosensor design. In our group, an original bienzymatic electrochemical sensing system was developed based on TK*ec* (in its apoenzyme form, apo-TK*ec*) and galactose oxidase (GAOx) immobilized on an electrode surface (Touisni et al.,

* Corresponding authors at: Clermont Université, Université Blaise Pascal, Institut de Chimie de Clermont-Ferrand, BP10448, F-63000 Clermont-Ferrand, France
E-mail addresses: Christine.MOUSTY@univ-bpclermont.fr (C. Mousty), Franck.CHARMANTRAY@univ-bpclermont.fr (F. Charmantray).

http://dx.doi.org/10.1016/j.bios.2016.09.049
Received 20 June 2016; Received in revised form 9 September 2016; Accepted 13 September 2016
Available online 14 September 2016
0956-5663/

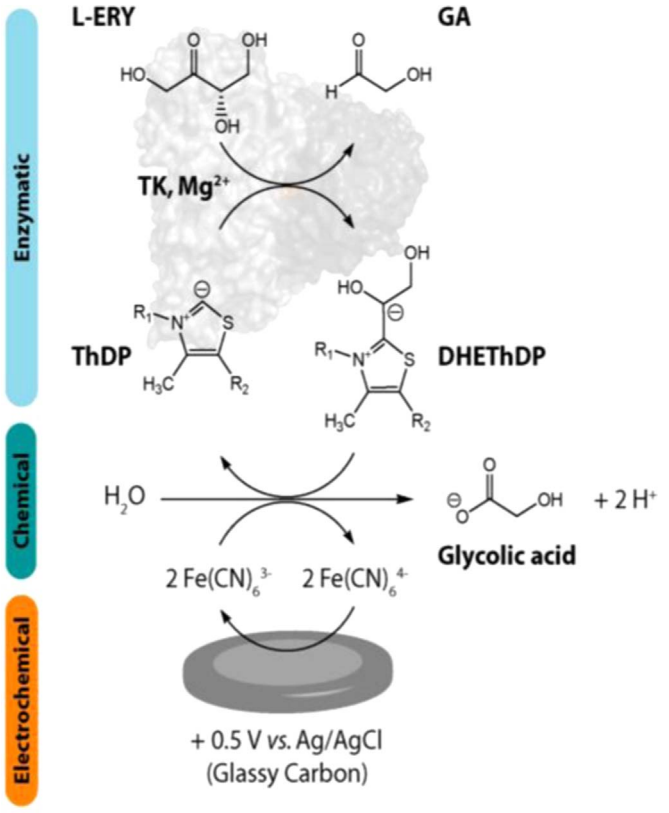

Scheme 1. Principle of thiamine electrochemical biosensor based on oxidative trapping of DHEThDP intermediate by hexacyanoferrate(III).

2014). In this analytical device, we used commercially available substrates, namely D-fructose-6-phosphate (D-F6P), a physiological donor and glycolaldehyde the best non-phosphorylated acceptor. Hence, GAOx allowed the amperometric detection of L-erythrulose (L-ERY) released upon TK-catalyzed reaction. This biosensor was validated with the determination of ThDP, the TK cofactor, and of TK inhibitors.

Interestingly, TK, which is not an oxidoreductase, is also able to catalyze a one-substrate reaction using a ketose (phosphate) as the donor substrate only (Bykova et al., 2001; Christen and Gasser, 1980; Fiedler et al., 2001). In the presence of TK cofactors (ThDP and Mg^{2+}) and when L-ERY is used as the donor substrate, TK leads to the concomitant formation of glycolaldehyde (GA) released after C-C bond cleavage of L-ERY, and α,β-dihydroxyethylthiamine diphosphate carbanion (DHEThDP) as the activated form of ThDP in the enzymatic active site (Scheme 1).

From an analytical point of view, this possibility of TK to work only with the donor substrate has been studied by Healy and Christen (1973), who managed to oxidize the DHEThDP intermediate using different redox mediators. When using hexacyanoferrate(III) as a redox mediator, the reaction leads to the formation of glycolic acid, ThDP and hexacyanoferrate(II). Providing that ThDP cofactor is regenerated, the catalytic reaction can proceed. The decrease in concentration of hexacyanoferrate(III) was followed by UV–Vis spectrophotometry at λ=420 nm (Christen and Gasser, 1980; Meshalkina et al., 2010; Usmanov and Kochetov, 1981).

In the present study, we propose to design an amperometric TK-based biosensor using the oxidative trapping of enzyme-substrate intermediate (DHEThDP). Indeed, hexacyanoferrate has been widely used as redox mediator in amperometric biosensing systems because of its reversible electrochemical behavior (Rawson et al., 2014). Therefore, hexacyanoferrate(III) is regenerated by the oxidation of hexacyanoferrate(II) released from the enzymatic reaction at the working electrode (E_{app}=+0.5 V vs Ag-AgCl) (Scheme 1).

A key step in the development of a biosensor is the immobilization of the enzyme at the electrode surface. Recently, in our group, the immobilization of TK into layered double hydroxides (LDH) was optimized (Benaissi et al., 2011; Touisni et al., 2013). These inorganic lamellar materials, also called anionic clays, exhibit intrinsic properties such as adsorption behavior, anionic exchange capacities and good biocompatibility, favorable for interactions with enzymes. These materials are also able to preserve the enzymes native integrity (Mousty and Leroux, 2012; Mousty and Prévot, 2013). TK*ec* was thus immobilized in its apoenzyme form, *i.e.* the enzyme devoid of its cofactors, on Mg_2Al-NO_3 LDH by the adsorption method to design a ThDP biosensor.

2. Experimental

2.1. Enzyme and reagents

Recombinant transketolase was expressed in *E. Coli* BL21 (DE3) containing the engineered plasmid pET21 harboring TKT1 gene from *E. Coli* with an N-terminal His_6 tag. TK*ec* was purified from the cell-free extract using a Ni-NTA resin from Qiagen as reported earlier (Touisni et al., 2013) (see Supporting Information). Purified TK was recovered in its apoenzyme form (apo-TK*ec*). (Hydroxyethyl)piperazine-1-ethanesulfonic acid (Hepes), glycyl-glycine (Gly-Gly), triethanolamine (TEA), D-fructose-6-phosphate (D-F6P), L-erythrulose (L-ERY), sodium pyruvate (PYR), thiamine pyrophosphate (ThDP), and alcohol dehydrogenase (ADH, 25 U mg^{-1}) and nicotinamide adenine dinucleotide (NADH) were purchased from Sigma-Aldrich. Magnesium and aluminum nitrate salts, $Mg(NO_3)_2{\cdot}6H_2O$ and $Al(NO_3)_3{\cdot}9H_2O$ and potassium hexacyanoferrate(III), $K_3Fe(CN)_6$, were of analytical grade (Acros Organics, Merck) and were used without further purification. Deionized water was used for all experiments.

2.2. TK activity determination by enzymatic assay

Enzymatic activity of TK*ec* was determined by a spectrophotometric assay at λ=340 nm, using a Cary 300 UV–visible spectrophotometer (Agilent), in the presence of L-ERY (85 mM) as donor and D-ribose-5-phosphate (8.9 mM) as acceptor substrate leading to D-sedoheptulose-7-phosphate and glycolaldehyde formation. The reaction was carried out in Gly-Gly buffer (50 mM, pH 7.5, 800 µL) with ThDP (106 µM, 10 mg mL^{-1}, 5 µL) and $MgCl_2$ (493 µM, 10 mg mL^{-1}, 10 µL) as cofactors. The TK activity was obtained by following the formation of ethylene glycol *via* consumption of NADH in the coupled enzymatic reaction with yeast alcohol dehydrogenase (2.5 U) as described before (Touisni et al., 2013, 2014). Lyophilized TK*ec* exhibited a specific activity of 16 U mg^{-1}.

2.3. Preparation of TKec/LDH modified glassy carbon electrodes

Adsorption of TK*ec* on Mg_2Al-NO_3 LDH nanoparticles was carried out by mixing the enzyme and the LDH suspensions. LDH nanoparticles were synthesized as previously described (Pavlovic et al., 2015; Xu et al., 2006) (see Supporting Information). A LDH suspension (10 mg mL^{-1}) was subsequently prepared in 10 mM Gly-Gly buffer solutions at pH 7.5 and left under stirring overnight. A TK*ec* suspension (30 mg mL^{-1}) was freshly prepared in the same Gly-Gly buffer. The adsorption was made instantly by mixing (25–75 µL) of LDH suspension and (8.3–25 µL) of TK*ec* suspension with a vortex to obtain TK*ec*/LDH ratios of 1:2 and 1:1 (w/w). The final volume of the mixtures of LDH and TK*ec* suspensions was fixed at 100 µL in Gly-Gly buffer.

The enzymatic activity of immobilized TK*ec* in biohybrid was also determined following the protocol described in Section 2.2. Colloidal suspensions of (TK*ec*/LDH 1:1 and 1:2) biohybrids were mixed in Gly-

Gly buffer in a UV–Vis cuvette (1 mL) with the other assay components and kept under stirring during the UV–Vis measurement. Knowing the amount of immobilized enzyme, the enzymatic activity of the biohybrids was compared to that obtained for the same amount of free TKec. These biohybrids exhibited an activity which corresponds to 92% and 91% of the initial activity of the free enzyme (14.7 U mg^{-1} of immobilized enzyme).

A drop (20 µL) of TK*ec*/LDH mixture, corresponding to 100, 200, 300 or 400 µg of biohybrid material, was deposited on the surface of a glassy carbon electrode (A=0.196 cm^2) and the bioactive layer was allowed to dry overnight at 4 °C. Before use, TK*ec*/LDH/GCE modified electrodes were rehydrated in Hepes buffer (pH=7.0, 50 mM) for 15 min and then transferred into the electrochemical cell to carry out chronoamperometric experiments (*vide infra*). The amount of TK*ec* immobilized on the electrode surface was calculated by the difference between the amount of protein initially adsorbed and the one detected in the washing buffer solution. The later value was determined by UV spectroscopy (λ=280 nm). Under the optimal conditions (300 µg), the amount of immobilized TK*ec* was 78%, 79% and 21% for respectively 1:1, 1:2 and 2:1 TK/LDH ratio. The repeatability of the fabrication of the TK*ec*/LDH/GCE biosensor (300 µg, 1:1) was tested with three different electrodes. The relative standard deviation (RSD) on the maximum intensity (I_{max} value, related to the amount of immobilized TK*ec*) was 8% for L-ERY determination. Control experiments were conducted using denatured TK after incubation of a TK*ec*/LDH/GCE modified electrode (300 µg, 1:1) in a Hepes buffer solution (pH 7.0, 50 mM) in a water bath at 60 °C for 1 h.

2.4. Procedures

2.4.1. Physical characterization of pristine LDH and TKec/LDH biohybrids

Pristine Mg_2Al-NO_3 LDH nanoparticles and TK*ec*/LDH biohybrids (1:1) were characterized using X-Ray diffraction (PXRD), Fourier-Transformed infrared spectroscopy (FTIR), Zeta-potential measurement and transmission electron microscopy (TEM). Powder X-ray diffraction patterns of inorganic materials were recorded on a Philips X-Pert Pro diffractometer equipped with a graphite monochromator using CuKα radiation (λ=0.15415 nm) over the 2.0–70.0° (2 θ) in steps of 0.033° with a counting time per step of 200 s. Infrared spectra (FTIR) were recorded with a Nicolet 5700 spectrometer from Thermo Scientific in transmission mode using the KBr pellet technique. Hydrodynamic particle size and Zeta-potentials of Mg_2Al-NO_3 and TK*ec*/LDH biohybrids were measured with a Zetasizer nano ZS (Malvern instruments) apparatus, using a laser Doppler electrophoresis (LDE) and compared to the values obtained for free TK*ec*. Transmission electron microscopy (TEM) images were taken using a Hitachi 7650 microscope at an acceleration voltage of 80 kV. One droplet of the aqueous colloidal suspension was applied to a 400 mesh holey carbon-coated copper grid and left to dry in air.

2.4.2. Electrochemical measurements

Cyclic voltammetry and chronoamperometry experiments were carried out with a potentiostat EA161 (EDAQ) connected to a thermostated cell (25 °C) with a three-electrode system. A saturated Ag-AgCl electrode was used as the reference electrode and a Pt wire as the counter electrode. The working electrode was the modified rotating disk glassy carbon electrode. Before TK*ec*/LDH biohybrids adsorption, the working electrode was polished with a diamond paste (1 µm) washed with acetone, then polished with alumina slurry (0.04 µm), and finally rinsed with ethanol and water. Before used the electrode was stabilized in 10 mL of 50 mM Hepes buffer solution (pH 7.5) containing 0.2 mM ThDP, 1 mM $MgCl_2$ and 1.0 mM $K_3Fe(CN)_6$ for 30 min. Cyclic voltammetry was performed at υ=5 mV s^{-1} without and in the presence of 1 mM L-ERY or D-F6P after 15 min of incubation. The same signal was obtained after 1 h.

The chronoamperometric measurements were performed in Hepes buffer solution containing 1.0 mM $MgCl_2$, 0.2 mM ThDP and 0.025, 0.10 or 1.0 mM $K_3Fe(CN)_6$ at an applied potential (E_{app}) of +0.5 V vs Ag-AgCl under steady state condition (500 rpm). After baseline stabilization under applied potential, the analyte concentrations to be assayed (here L-ERY, D-F6P and PYR) were increased stepwise by recurrent additions of concentrated stock solutions using a micropipette. The current response was measured after its stabilization. The response time (t_{90}) was determined as the time required to reach 90% of the current response. The same procedure was also performed with a biosensor containing denatured TK*ec* (control experiment), using L-ERY as substrate. The stability of a TK*ec*/LDH modified electrode was carried out by soaking in Hepes buffer solution (pH 7.0, 50 mM) at 4 °C for 12 days. The mean response of the biosensor over this period of time was obtained after 3 successive additions of 1 mM L-ERY.

The ThDP assays were carried out following two protocols using an electrolyte solution without ThDP (Hepes buffer 50 mM pH 7.5, 1.0 mM $MgCl_2$). After baseline stabilization at E_{app}=0.5 V vs Ag-AgCl, D-F6P was then added at once for a final concentration of 1 mM. This step was followed by stepwise additions of ThDP from concentrated stock solution as explained before. The current response was measured during 15 min after each ThDP additions. In parallel, six different TK*ec*/LDH/GCE biosensors were tested after baseline stabilization under E_{app} in the presence of ThDP at different concentrations between 1 µM–10 µM. The chronoamperometric responses were recorded after 1 mM D-F6P addition.

The calibration curves of L-ERY, D-F6P, PYR and ThDP were done in triplicate. The linear range of the calibration plots was fixed according to the best correlation coefficient ($R^2 > 0.980$); the sensitivity (S) was expressed as the slope of the calibration curve. The limit of detection (LOD) was defined as a signal-to-noise ratio of 3 and I_{max} corresponded to the pseudo-plateau observed in the calibration curves.

3. Results and discussion

The immobilization of TK*ec* in its apoenzyme form onto the electrode surface is of particular interest in the development of a biosensor. Recently we have shown that the immobilization of TK*ec* can be carried out using LDH as immobilization matrix by two processes: adsorption and coprecipitation (Touisni et al., 2013). In the present study, the former method is optimized using LDH nanoparticles in order to favor the accessibility of TK*ec* active site and hence to reduce the response time of the biosensors.

3.1. Preparation and characterization of TKec/LDH biohybrids

LDH are lamellar materials based on the stacking of positively charged sheets $[M^{II}_{1-x}M^{III}_{x}(OH)_2]^{x+}$; anions and water molecules are located in the interlamellar domain to maintain the overall electroneutrality (Forano et al., 2013). Mg_2Al-NO_3 nanoparticles LDH were synthesized by a fast coprecipitation followed by hydrothermal treatment (see Supporting Information), whereby a stable colloidal suspension was obtained (Pavlovic et al., 2015; Xu et al., 2006). Considering the isoelectric point of TK*ec* (IP =6.3), electrostatic interactions with the positively charged layers of LDH are promote at the optimum pH value of this enzyme (7.5) (Touisni et al., 2013). Indeed at this pH, the enzyme displays an overall negative charge with a zeta-potential of −32 mV in 10 mM Gly-Gly buffer at pH 7.5. The adsorption process was therefore achieved in these conditions, the TK*ec*/LDH ratio being fixed at 1:1 and 1:2 (w/w). After adsorption, the zeta potential of TK*ec*/LDH biohybrid was found around −17 mV and −15 mV and the percentage of TK*ec* adsorption was estimated at 78% and 79%, respectively for 1:1 and 1:2 ratio. The activities of these biohybrids (TK*ec*/Mg_2Al-NO_3 1:1 and 1:2) in suspensions correspond respectively

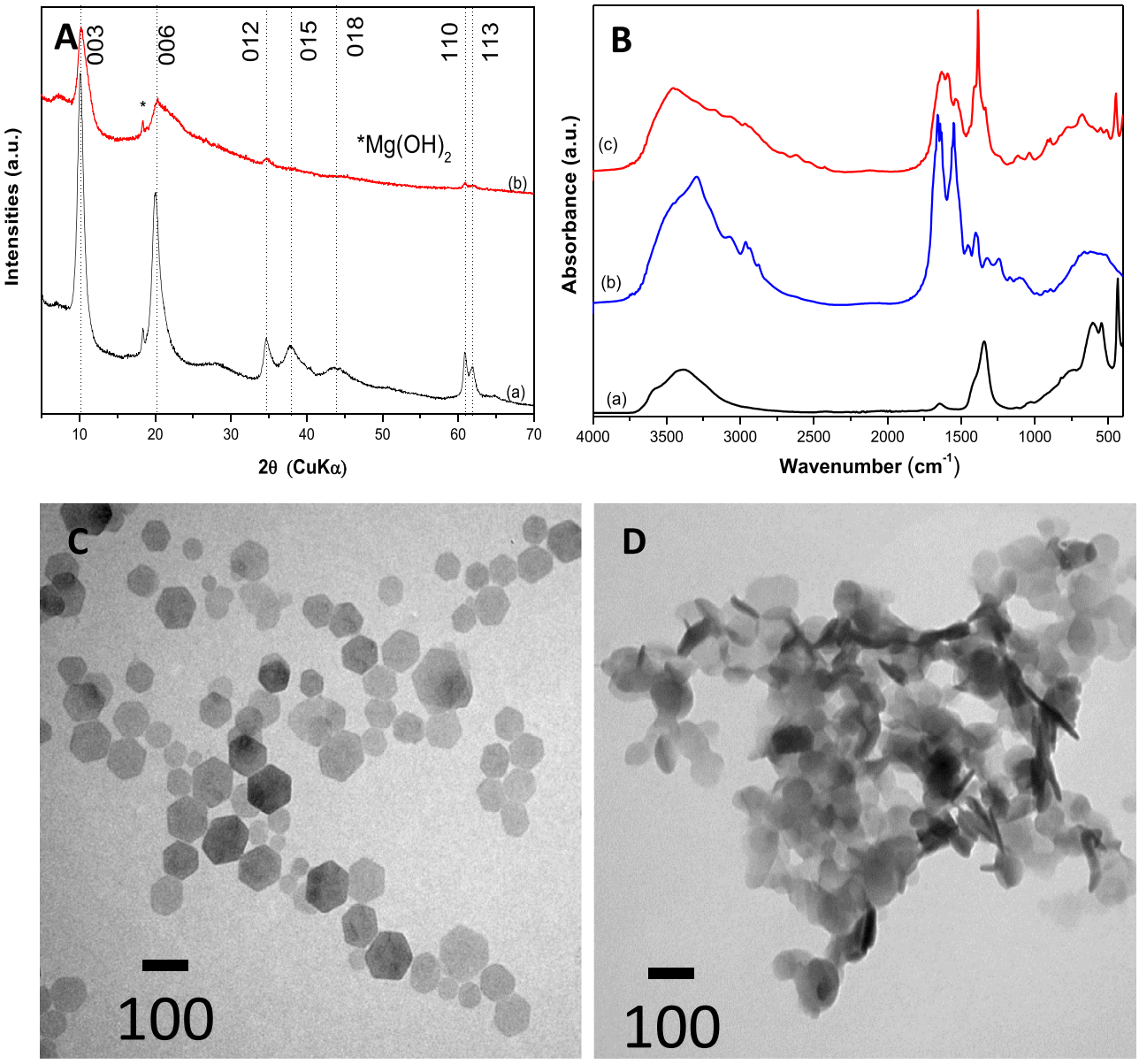

Fig. 1. (A) PXRD patterns of pristine $Mg_2Al\text{-}NO_3$ LDH (a) and TK*ec*/LDH (1:1) (b); (B) FTIR spectra of pristine $Mg_2Al\text{-}NO_3$ LDH (a), TK*ec* enzyme (b) and TK*ec*/LDH biohybrid (c); (C) and (D) TEM images of respectively $Mg_2Al\text{-}NO_3$ LDH and TK*ec*/LDH (1:1).

to 92% and 91% of the initial activity of the free enzyme. As a comparison, the adsorption of TK*ec* in a cationic clay, namely the laponite (1:1 and 1:2) leads to 60% and 70% of adsorption respectively and with less than 15% of initial enzymatic activity, confirming the benefit of using LDH as the immobilization matrix.

The X-ray pattern of TK*ec*/LDH biohybrid material displays strongly-enlarged diffraction lines, as well as a decrease of (00*3* and 00*6*) diffraction line intensity (Fig. 1A(b)), evidencing the influence of adsorbed TK*ec* on the structural and textural properties of the LDH. These PXRD pattern modifications can be attributed to an increase of disorder into the layer stacking (Benaissi et al., 2011; Touisni et al., 2013). However, the diffraction lines pointed at the same positions that the pristine LDH, revealing the effective bearing of the LDH layered structure after TK*ec* immobilization. The position of the (00*3* and 00*6*) diffraction lines of LDH before and after TK*ec* adsorption remained unchanged, proving that TK*ec* did not intercalate in the LDH structure as expected due to its large size (9 nm) (Jahromi et al., 2011; Touisni et al., 2013); nitrate anions still being the intercalated species after the adsorption process. Enzyme adsorption was further evidenced on FTIR spectrum (Fig. 1B(c)). Pure TK*ec* spectrum showed enzyme characteristic vibrations as bands or shoulders at 3066 – 2873 cm^{-1} (ν_{CH2}, ν_{CH3}); 1658 cm^{-1} (ν_{CO} – amide I); 1546 cm^{-1} (δ_{NH} and ν_{CN} – amide II) and 1242 cm^{-1} (ν_{NH}, ν_{CN} – amide III) (Fig. 1B(b)). For the TK*ec*/LDH biohybrid material, some vibration bands of both TK*ec* enzyme and LDH matrix were identified, suggesting both LDH and TK*ec* presence into the biomaterial formed by the adsorption method. TEM image of TK*ec*/LDH colloidal suspension clearly evidenced the influence of TK*ec* adsorption on LDH nanoparticles. Rather than individual platelets observed for pristine LDH, the electrostatic interaction between positively charged LDH layers and negatively charged TK*ec* induces particles aggregation (Fig. 1D) due to surface charge neutralization. It is noteworthy that adsorption process also leads to a slight modification of the LDH nanoparticles shape which may be due to a partial hydrolysis of the surface. Interestingly, the adsorption process does not affect the TK*ec* enzymatic activity which retains 92% of its initial activity for an enzyme /LDH ratio of 1:1.

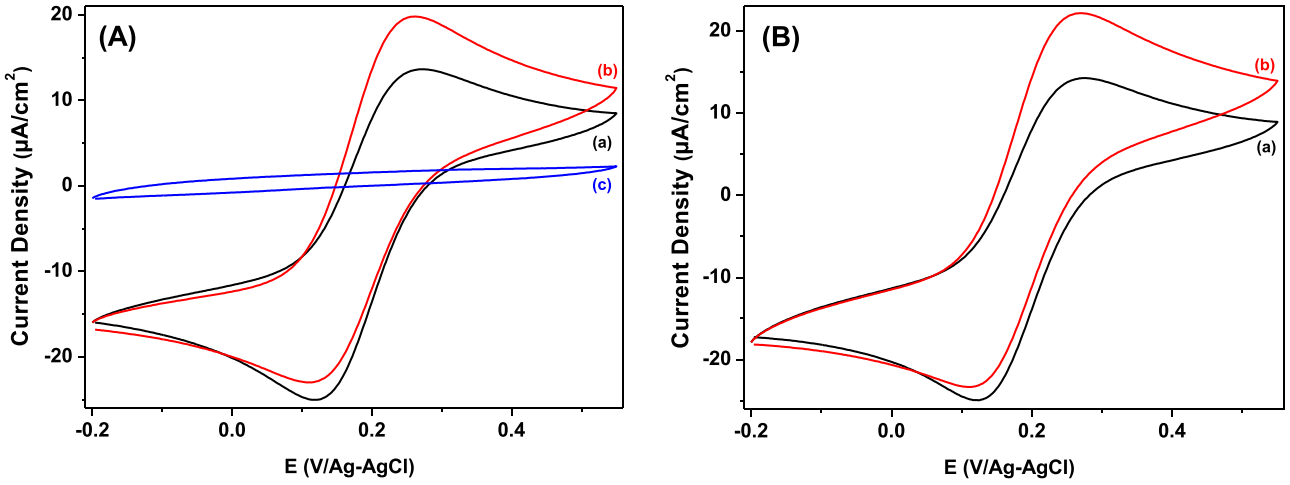

Fig. 2. Cyclic voltammograms of TK*ec*/LDH (1:1, 300 μg) in 1 mM $K_3Fe(CN)_6$ before (a) and after (b) addition of 1 mM L-ERY (A) and D-F6P (B). Curve (c) shows the baseline of the TK*ec*/LDH in absence of $K_3Fe(CN)_6$. Experimental conditions: 50 mM Hepes pH 7.5 at 25 °C, 0.2 mM ThDP, 1 mM $MgCl_2$, v=5 mV s^{-1}.

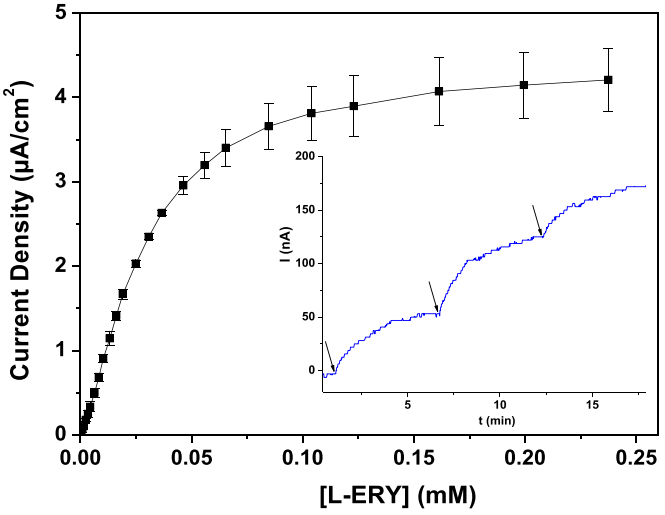

Fig. 3. Calibration curve of L-ERY recorded with TK*ec*/LDH/GCE (300 μg, 1:1) biosensor using 1.0 mM $K_3Fe(CN)_6$. Inset: Chronoamperometric response of TK*ec*/LDH/GCE biosensor adding 3 μM L-ERY in the presence of 1 mM $K_3Fe(CN)_6$. Experimental conditions: 50 mM Hepes pH 7.5 at 25 °C, 0.2 mM ThDP, 1 mM $MgCl_2$, E_{app}=+ 0.5 V/Ag-AgCl, 500 rpm.

3.2. Optimization of TK*ec*/LDH/GCE biosensor

An original amperometric transduction process was optimized with this monoenzymatic TK*ec*/LDH/GCE biosensor. It was based on the ability of hexacyanoferrate(III) to oxidize the enzyme-substrate intermediate (DHEThDP) to GA along with ThDP regeneration (Christen and Gasser, 1980). The apo-TK*ec* in the TK*ec*/LDH/GCE biosensor needs to be activated by its cofactors, ThDP and $MgCl_2$ in 50 mM Hepes buffer solution (pH 7.5). The voltammetric curves clearly showed the modification of the electrochemical signal of $Fe(CN)_6^{3-}$ upon the electroenzymatic reaction with an increase of the anodic peak in the presence of the donor substrates, namely L-ERY and D-F6P (Fig. 2). Furthermore, the curve c shows that no oxidation peak was observed in the presence of ThDP, Mg^{2+} and L-ERY.

The increase of the amperometric signal measured under steady state condition at +0.5 V/Ag-AgCl corresponds to the oxidation of $Fe(CN)_6^{4-}$ formed in the carbanion oxidative trapping step (Scheme 1). The TK*ec*/LDH/GCE biosensor was optimized using a best TK*ec* donor substrate, namely L-ERY (Besse et al., 1997; Schenk et al., 1998). The experiments were carried out using a series of modified electrodes with a 1:1 TK*ec*/LDH ratio and 300 μg of biohybrid, which corresponds to 117 μg (1.7 U) of immobilized TK*ec*.

3.2.1. Hexacyanoferrate(III) concentration

The influence of hexacyanoferrate(III) concentration on TK*ec*/LDH/GCE biosensor response was first investigated, since, it was reported earlier (Christen et al., 1976; Yurshev et al., 2010) that hexacyanoferrate(III) may cause TK inhibition. The TK activity in solution was first determined after incubation (30 min) in the presence of 0.1–1 mM $K_3Fe(CN)_6$ in Gly-Gly buffer (50 mM, pH 7.5) containing 0.5 mM of $MgCl_2$ and 0.1 mM of ThDP. Under our experimental conditions, only 9%, 10% and 13% of TK*ec* inhibition were observed in the presence of 0.1, 0.5 and 1 mM $K_3Fe(CN)_6$, respectively. Hence, we assumed that this slight inhibition of TK*ec* did not prevent further experiments on TK*ec*/LDH/GCE biosensor to be carried out straightforwardly. However the maximum concentration of $K_3Fe(CN)_6$ tested was limited to 1 mM, which corresponds to 13% inhibition only.

Typical amperometric responses upon 3 μM L-ERY additions for 1 mM $K_3Fe(CN)_6$ are shown in Inset of Fig. 3. L-ERY calibration curves were obtained in the presence of three different $K_3Fe(CN)_6$ concentrations into the electrolyte, namely 0.025, 0.1 (data not shown) and 1.0 mM (Fig. 3). The resulting biosensor characteristics, *i.e.* sensitivity (S), maximum current density (I_{max}), and the dynamic concentration range (LR) are given in Table SI.1, showing a positive effect of

Table 1
Amperometric performances of TK*ec*/LDH/GCE (300 μg, 1:1) biosensor for TK*ec* substrates determination in 50 mM Hepes pH 7.5 at 25 °C, 0.2 mM ThDP, 1 mM $MgCl_2$, 1 mM $K_3Fe(CN)_6$, E_{app}=+0.5 V/Ag-AgCl, 500 rpm.

Substrate	LOD (μM)	Linear range (μM)	Sensitivity (mA M^{-1} cm^{-2})	RSD (%)	I_{max}μA cm^{-2}	RSD (%)	R^2 (n)
L-ERY	1.0	1–19	90	1.2	4.2	8.2	0.999 (11)
D-F6P	1.5	1–37	55	2.5	4.6	5.4	0.999 (14)
PYR	4.5	1.5–13	18	1.6	1.1	0.5	0.969 (8)
ThDP[a]	0.02	0.02–0.4	3831	19	4.4	16	0.998 (9)

[a] 1 mM of D-F6P.

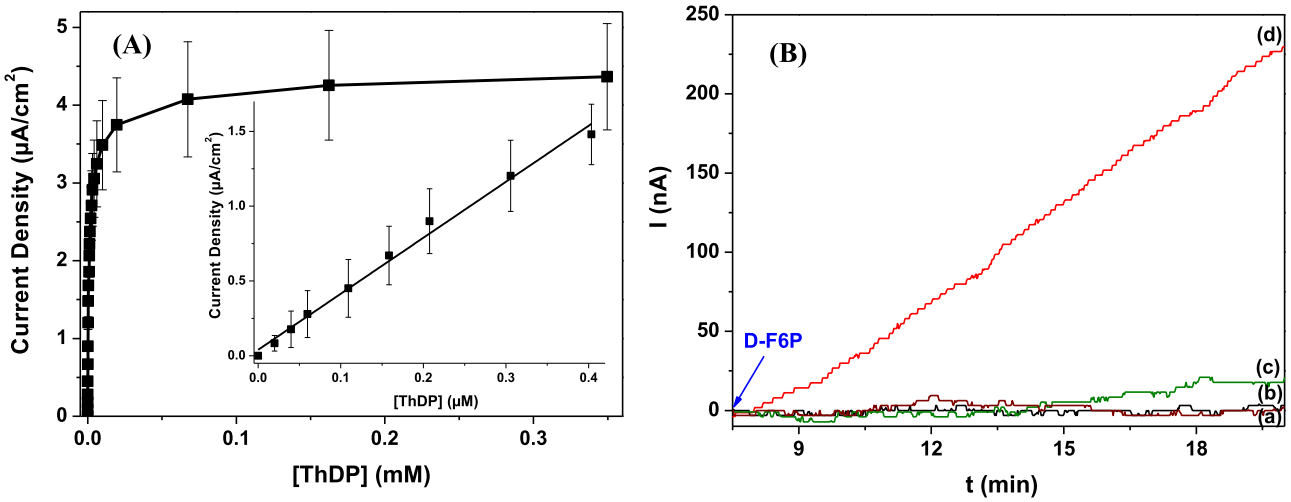

Fig. 4. (A) Calibration curve obtained for successive additions of ThDP at a TKec/LDH GCE biosensor. Inset: Linear range of ThDP. (B) Chronoamperometric response for 1 mM D-F6P recorded with TKec/LDH/GCE biosensors incubated for 45 min in 10 μM of thiamine monophosphate (a); oxythiamine (b); thiamine (c) and ThDP (d). Experimental conditions: 50 mM Hepes pH 7.5 at 25 °C, 1 mM $MgCl_2$, 1 mM $K_3Fe(CN)_6$, 1 mM D-F6P, E_{app}=+0.5 V vs Ag-AgCl, 500 rpm.

increasing concentration of $K_3Fe(CN)_6$ on the biosensor response. Using 0.1 mM $K_3Fe(CN)_6$, the sensitivity of the biosensor for L-ERY reached 59 mA M^{-1} cm^{-2}, while it was only 48 mA M^{-1} cm^{-2} with 0.025 mM and it even increased to 90 mA M^{-1} cm^{-2} at 1 mM.

Similarly, the observed I_{max} value increased by a factor 3 between 0.025 mM and 0.1 mM to reach a value of 4.0 μA cm^{-2} with 1.0 mM $K_3Fe(CN)_6$. All these results together prompted us to set $K_3Fe(CN)_6$ concentration at 1.0 mM.

3.2.2. TKec/LDH/GCE biosensor composition

In order to determine the effect of enzyme loading and the best biohybrid composition on the biosensor response, we have studied three different TK*ec*/LDH ratios 1:1, 1:2 and 2:1 for a total amount of TK*ec*/LDH biohybrid of 300 μg on the electrode surface and four different amounts of biohybrid, *i.e.* 100, 200, 300 and 400 μg for a fixed TK*ec*/LDH ratio 1:1 (Table SI.1). We observed 20% of protein leaching for TK*ec*/LDH ratios 1:1 and 1:2 and even ≈80% for 2:1 ratio. Thus the TK*ec*/LDH biohybrid 2:1 was discarded due to protein overload as evidenced earlier (Touisni et al., 2013).

As expected, a lower amount of immobilized enzyme (ratio 1:2, 79 μg) gave a lower I_{max} value and a smaller dynamic concentration range, whereas the sensitivity remained the same as that obtained with TK*ec*/LDH ratios of 1:1 (117 μg). Concerning the amount of TK*ec*/LDH biohybrid deposited on the electrode surface, up to 300 μg biohybrid, both the sensitivity and the I_{max} increased. Above (400 μg), I_{max} still increased while sensitivity decreased. I_{max} increase might be linked with the total amount of active enzyme immobilized, whereas S decrease might be due to the thickness of the biohybrid layer that might prevent efficient analyte and $Fe(CN)_6^{3-}$ diffusion. Thus, a 300 μg amount of TK*ec*/LDH 1:1 biohybrid was chosen for the optimized biosensor configuration.

3.2.3. Reuse and long-term stability of the biosensor

Experiments were performed to monitor the TK*ec*/LDH/GCE biosensor reusability and its stability over a long period of time. A single TK*ec*/LDH/GCE biosensor was used repeatedly (3 times in the same day) with 1 mM L-ERY giving the same current response (37 nA ± 4 nA) indicating the good performances of the biosensor for efficient reuse. Another TK*ec*/LDH/GCE biosensor was used once, washed and stored in Hepes buffer at 4 °C, between each measurement carried out in day 1, 2, 5 and 12. After 5 days, the biosensor retained about 75% of its initial activity and 28% after 12 days. Based on these results, TK*ec*/LDH/GCE biosensor could be reused several times on the day and could be stored up to 5 days with good performances. Finally, a control experiment was carried out using denatured TK*ec*. The response was found to be in the range of the background signal (Fig. SI.1a). Moreover, with an active TK*ec*/LDH/GCE, the amperometric signal remains unchanged when ThDP was added in substrate absence (Inset Fig. SI.1). These control experiments confirm that the TK*ec* enzyme is mandatory for the efficient working of the TK*ec*/LDH/GCE biosensor and that ThDP or the substrate alone does not interfere in the amperometric response.

3.3. Detection of TK donor substrates

The optimized TK*ec*/LDH/GCE biosensor was then tested with the best TK*ec* donor substrates, namely L-ERY and D-F6P (Besse et al., 1997; Schenk et al., 1998). We also assayed PYR, as an extremely poor donor substrate of TK (Schneider and Lindqvist, 1998). All experiments were performed, using three different electrodes, under the same conditions. As expected, some higher TK*ec*/LDH biosensor performances were observed with the best TK*ec* donor substrates (L-ERY and D-F6P) than for PYR (Fig. SI.1). The response-time curves observed for the three substrates tested were as follows: t_{90}=1.2 min for L-ERY; t_{90}=3 min for D-F6P and t_{90}=3.3 min for PYR. The linear range of the D-F6P calibration plot was fixed according to a correlation coefficient R^2=0.999 (n=14). Similar linear ranges were obtained for L-ERY and PYR (Table 1). The average value of sensitivity (S) and maximum current density (I_{max}) with relative standard deviation (RSD) are also presented in Table SI.1. L-ERY was assayed with the best sensitivity (90 mA M^{-1} cm^{-2}), it was followed by D-F6P (55 mA M^{-1} cm^{-2}) and eventually PYR (18 mA M^{-1} cm^{-2}), which was possible to clearly distinguish from background noise experiment. The calculated limits of detections (LOD) were around 1.5 μM for D-F6P, 1.0 μM for L-ERY and 4.5 μM for PYR. The maximum current density (I_{max}), was found to be 4.6 μA cm^{-2} for D-F6P; 4.2 μA cm^{-2} for L-ERY and only 1.1 μA cm^{-2} for PYR. Contrary to L-ERY and D-F6P that possess a ketol group, PYR does not, and as a consequence, it behaves as a poor donor substrate of TK*ec*. D-F6P and L-ERY are known as very good TK donor substrates. D-F6P (along with D-Xylulose-5-phosphate) is even described as the best TK donor substrate (*Km*=1.1 mM; *Vmax*=62 U mg^{-1};*Vmax*/ *Km*=56 U mg^{-1} mM^{-1}) (Sprenger et al., 1995). L-ERY behaves as a good TK donor substrate and is considered the best unphosphorylated TK donor substrate (*Km*=18 mM; *Vmax*=12 U mg^{-1}; *Vmax*/ K_M=0.7 U mg^{-1} mM^{-1}) (Abdoul-Zabar et al., 2013). However, despite their kinetic constants, we observed both a better

sensitivity and lower detection limit for the L- ERY (S=90 mA M^{-1} cm^{-2} and LOD=1.0 μM) compared to the D-F6P (S=55 mA M^{-1} cm^{-2} and LOD=1.5 μM). This might be issued from the interaction of D-F6P that is negatively charged and acidic with the LDH matrix.

The performance of TK*ec*/LDH/GCE biosensor for L-ERY assays was compared to that reported for another galactose oxidase (GAOx) biosensor (Touisni et al., 2014). Even though L-ERY is a good substrate of GAOx, the sensitivity in the latter case was lower (48 mA M^{-1} cm^{-2} *vs* 90 mA M^{-1} cm^{-2}). Similarly, Usmanov and Kochetov (1981) described an UV–Vis assay using TK from *baker's yeast* and hexacyanoferrate(III) in solution for D-F6P determination at 15 and 53 μM. In comparison with our amperometric biosensor, the UV–Vis experiment required a relative large amount of TK (380 μg) and the lowest D-F6P concentration was found 10 times higher (15 μM) than those obtained by amperometry (1.5 μM). These results show that the oxidative trapping of enzyme-substrate intermediate coupled with an amperometric transduction process is promising for biosensor device.

3.4. Detection of thiamine diphosphate (ThDP)

As referred in several studies mentioned in the introduction, there is a tremendous interest to develop a simple, stable and mostly sensitive device to detect thiamine (vitamine B1) since a deficiency or excess in the body interfere in the activity of key enzymes that triggers serious diseases. For this purpose, efforts were conducted to optimize the TK*ec*/LDH/GCE biosensor, in particular to determine ThDP concentrations, as the TK*ec* cofactor. Hence, activation of immobilized apo-TK*ec* requires its complexation with ThDP. To mimic the reaction that takes place *in vivo*, D-F6P was employed as a natural donor substrate of TK*ec*.

Several biosensors were first tested independently after baseline stabilization under E_{app} in different electrolyte solutions containing low concentration of ThDP (1–10 μM). Interestingly, the I *vs* t slope of the initial reaction rate (t < 20 min) depends on the ThDP concentration (Fig. SI.2). Noticeably, at low ThDP concentration, ThDP binding in the TK active site is the limiting step reaction in the whole electroenzymatic cascade. Therefore, a calibration curve was established by measuring the current response after 15 min following each ThDP addition in an electrolyte solution containing 1 mM D-F6P (Fig. 4). Under this condition, a linear range of the calibration plots was established between 2.0×10^{-8}–4.0×10^{-7} M ThDP with a LOD of about 20 nM and a mean sensitivity for three different biosensors of 3831 mA M^{-1} cm^{-2} (Table 1). The maximum current density (I_{max}) value was close to the value obtained for the calibration curve of the donor substrate of TK*ec* (D-F6P). Interestingly, it was observed an exalted sensitivity (S=3831 mA M^{-1} cm^{-2}), at least 50 times more sensible than the previously found, by using a bi-enzymatic TK*ec*-GaOx biosensor (Touisni et al., 2014).

The kinetic parameters of ThDP *Km*(and *Vmax*) were determined for TK*ec*/LDH biohybrid using the standard Michaelis–Menten model and compared with those obtained for the free TK*ec*. For the free enzyme, those kinetics parameters were determined by two methods: i) by spectrophotometry at λ=420 nm with D-F6P as TK donor substrate in presence of $K_3Fe(CN)_6$ as redox mediator; ii) by spectrophotometry at λ=340 nm using a donor substrate (L-ERY) and an acceptor substrate (D-ribose-5-phosphate) in the presence of NADH and ADH (Alcohol dehydrogenase). The results obtained following the Hanes-Woolf double reciprocal plots are summarized in Table SI.2. The *Km* of ThDP for TK*ec* was found to be identical. Indeed, the *Km* value for TK*ec* after immobilization in LDH (*Km*=1.6 μM) is very close to the value obtained for free TK*ec* (Km=1.80 or 2.75 μM depending on the method of determination). This result proves that LDH does not interfere in the interaction between ThDP and TK*ec*. On the contrary, catalytic efficiency (*Vmax*/*Km*) seems to be improved when the enzyme was immobilized in the LDH matrix.

We have also carried out an ultimate experiment to investigate the selectivity of TK*ec*/LDH/GCE for ThDP amongst different ThDP analogs namely oxythiamine, thiamine and thiamine monophosphate (10 μM). For this purpose, experiments were done under the same experimental conditions employed for ThDP assay. The result obtained was unambiguous in the sense that ThDP, and ThDP only, led to a 20 nA min^{-1} increase in current intensity once the reaction was started (D-F6P addition) (Fig. 4B). This result demonstrates the excellent selectivity of TK*ec*/LDH/GCE for ThDP that may result in the high affinity of TK*ec* for its cofactor ThDP. A maximum response was observed when 0.2 mM of ThDP was added, after 20 min, in presence of thiamine monophosphate (Fig. SI.3). Similar results were obtained whatever the ThDP analog assayed (data not shown).

4. Conclusion

A powerful mono-enzymatic biosensor for ThDP detection was designed using enzyme TK*ec* immobilized in LDH material. Biosensor responses were measured using an original system based on the oxidative trapping of TK-intermediate (DHEThDP) at a TKec/LDH modified glassy carbon electrode in presence of the hexacyanoferrate (III). TK*ec*/LDH/GCE biosensor was easily prepared and displayed outstanding sensitivity and reproducibility for different donor substrates of the enzyme. Extra, this biosensor showed potency to detect the thiamine (ThDP) with excellent sensitivity, which is mandatory for an *in vivo* thiamine detection device. For practical applications purpose, further improvements are required. One could for example decrease the response time by using another redox mediator. This work is currently under investigation. Finally, we anticipate that other biosensors based ThDP-dependent enzymes may be developed using the same concept of signal transduction.

Acknowledgments

The authors would like to thank the French ANR agency for its financial support (ANR- 13-JSV5-0002-01 Transbioscreen).

Appendix A. Supporting information

Supplementary data associated with this article can be found in the online version at doi:10.1016/j.bios.2016.09.049.

References

Abdoul-Zabar, J., Sorel, I., Hélaine, V., Charmantray, F., Devamani, T., Yi, D., de Bernardins, V., Louis, D., Marlière, P., Fessner, W.-D., Hecquet, L., 2013. Adv. Synth. Catal. 355, 116–128.
Ahopelto, K., Böckelman, C., Hagström, J., Koskensalo, S., Haglund, C., 2016. Cancer Biol. Ther. 17, 163–168.
Akyilmaz, E., Yorganci, E., 2008. Biosens. Bioelectron. 23, 1874–1877.
Akyilmaz, E., Yaşa, I., Dinçkaya, E., 2006. Anal. Biochem. 354, 78–84.
Basiri, B., Sutton, J.M., Hanberry, B.S., Zastre, J.A., Bartlett, M.G., 2016. Biomed. Chromatgr. 30, 35–41.
Benaissi, K., Hélaine, V., Prévot, V., Forano, C., Hecquet, 2011. Adv. Synth. Catal. 353, 1497–1509.
Bentz, S., Cee, A., Endlicher, E., Wojtal, K.A., Naami, A., Pesch, T., Lang, S., Schubert, P., Fried, M., Weber, A., Coy, J.F., Goelder, S., Knüchel, R., Hausmann, M., Rogler, G., 2013. Digestion 88, 182–192.
Besse, P., Bolte, J., Demuynck, C., Hecquet, L., Veschambre, H., 1997. Recent Res. Dev. Org. Chem., 191–228.
Butterworth, R.F., 2003. Nut. Res. Rev. 16, 277–283.
Bykova, I.A., Solovjeva, O.N., Meshalkina, L.E., Kovina, M.V., Kotchetov, G.A., 2001. Biochem. Biophys. Res. Commun. 280, 845–847.
Christen, P., Gasser, A., 1980. Eur. J. Biochem. 107, 73–77.
Christen, P., Cogoli-Greuter, M., Healy, M.J., Lubini, D., 1976. Eur. J. Biochem. 63, 223–231.
Du, M.X., Sim, J., Fang, L., Yin, Z., Koh, S., Stratton, J., Pons, J., Wang, J.J.-X., Carte, B., 2004. J. Biomol. Screen. 9, 427–433.
Fiedler, E., Golbik, R., Schneider, G., Tittmann, K., Neef, H., König, S., Hübner, G., 2001. J. Biol. Chem. 276, 16051–16058.
Forano, C., Costantino, U., Prevot, V., Taviot-Gueho, C., 2013. Handbook of Clay Science. Second edition, Vol Developments in Clay Science 5A, Elsevier, pp. 745–782.
Hanninen, S.A., Darling, P.B., J. Sole, M.J., Barr, A., Keith, M.E., 2006. J. Am. Coll.

Cardiol. 47, 354–361.
Healy, M.J., Christen, P., 1973. Biochemistry 12, 35–41.
Isenberg-Grzeda, E., Kutner, H.E., Nicolson, S.E., 2012. Psychosom. 53, 507–516.
Jahromi, R.R.F., Morris, P., Martinez-Torres, R.J., Paul, A., Dalby, A., 2011. J. Biotechnol. 155, 209–216.
Karuppagounder, S.S., Xu, H., Shi, Q., Lian, H., Chen, L.H., Pedrini, S., Pechmana, D., Baker, H., Beal, M.F., Gandy, S.E., Gibson, G.E., 2009. Neurobiol. Aging 30, 1587–1600.
Li, X., Song, J., Wang, Y., Cheng, T., 2013. Anal. Chim. Acta 797, 95–101.
Lonsdale, D., 2006. Adv. Access Pub. 3, 49–59.
Meshalkina, L.E., Solovjeva, O.N., Khodak, Y.A., Drutsa, V.L., Kotchetov, G.A., 2010. Biochemistry 75, 873–880.
Michalak, S., Michałowska-Wender, G., Adamcewicz, G., Wender, B.G., 2013. Folia Neuropath. 51, 222–226.
Mocali, A., Della Malva, N., Abete, C., Costanza, V.A.M., Bavazzano, A., Boddi, V., Sanchez, L., Dessì, S., Pani, A., Paoletti, F., 2014. Int. J. Alzheimer's Dis. 2014, 1–8.
Moghaddam, A.B., Gudarzy, F., Ganjkhanlou, Y., 2014. J. Fluoresc. 24, 1025–1030.
Mousty, C., Leroux, F., 2012. Recent Pat. Nanotechnol. 6, 174–192.
Mousty, C., Prévot, V., 2013. Anal. Bioanal. Chem. 405, 3513–3523.
Oni, J., Westbroek, P., Nyokong, T., 2002. Electroanalysis 14, 1165–1168.
Parsaei, P., Bahmaei, M., Ghannadi, A.R., 2014. Iran. J. Pharm. Res. 13, 1437–1445.
Parshina, A.V., Bobreshova, O.V., 2014. Pet. Chem. 54, 631–636.
Pavlovic, M., Sipiczki-Adok, M., Vebert, C., Pearson, S., Bourgeat-Lami, E., Prevot, V., Szilagyi, I., 2015. Langmuir 31, 12609–12617.
Poongothai, S., Ilavarasan, R., Karrunakaran, C.M., 2010. Int. J. Pharm. Pharm. Sci. 2, 133–139.
Rahman, S.T.A., Elbashir, A.A., El-Mukhtar, M., Ibrahim, M.M., 2015. Enliven: Bio. Anal. Tech. 2, 1–6.
Ranoux, A., Hanefeld, U., 2013. Top. *Catal.* 56, 750–754.
Rawson, F.J., Downard, A.J., Baronian, K.H., 2014. Sci. Rep. 4, 1–9.
Schenk, G., Duggleby, R.G., Nixon, P.F., 1998. Int. J. Biochem. Cell Biol. 30, 1297–1318.
Schneider, G., Lindqvist, Y., 1998. Biochim. Biophys. Acta 1385, 387–398.
Smithline, H.A., Donnino, M., Greenblatt, D.J., 2012. BMC Clin. Pharmacol. 12, 1–10.
Sprenger, G.A., Schörken, U., Sprenger, G., Sahm, H., 1995. Eur. J. Biochem. 230, 525–532.
Tan, H., Li, Q., Zhou, Z., Ma, C., Song, Y., Xu, F., Wang, L., 2015. Anal. Chim. Acta 856, 90–95.
Touisni, N., Charmantray, F., Helaine, V., Hecquet, L., Mousty, C., 2014. Biosens. Bioelectron. 62, 90–96.
Touisni, N., Charmantray, F., Helaine, V., Forano, C., Hecquet, L., Mousty, C., 2013. Colloids Surf. B 112, 452–459.
Tyszczuk-Rotko, K., 2012. Food Chem 134, 1239–1243.
Usmanov, R.A., Kochetov, G.A., 1981. Biochem. Int. 3, 33–39.
Wan, Q., Yang, N., Ye, Y., 2002. Anal. Sci. 18, 413–416.
Wang, X., Wang, B., Fan, Z., Shi, X., Ke, Z.-J., Luo, J., 2007. Neurosci. 144, 1045–1056.
Xu, M.-J.I., Lai, K.-H.R., Lin, S.-H., Tse, P.-W.A., Chiu, K.-C.D., Koh, H.-Y., Law, C.-T., Wong, C.-M., Cai, Z., Wong, C.-L.C., Ng, O.-L.I., 2016. PNAS 6, 725–734.
Xu, Z.P., Stevenson, G., Lu, C.Q., Lu, G.Q., 2006. J. Phys. Chem. B 110, 16923–16929.
Yurshev, V.A., Sevostyanova, I.A., Solovjeva, O.N., Kochetov, G.A., 2010. Biochemistry 75, 1014–1016.
Zhao, J., Zhong, C.-J., 2009. Neurosci. Bull. 25, 94–99.